

# Noble gases identify the mechanisms of fugitive gas contamination in drinking water wells overlying the Marcellus and Barnett Shales

Thomas H. Darrah<sup>a,b,1</sup>, Avner Vengosh<sup>a</sup>, Robert B. Jackson<sup>a,c</sup>, Nathaniel R. Warner<sup>a,d</sup>, and Robert J. Poreda<sup>e</sup>

<sup>a</sup>Division of Earth and Ocean Sciences, Nicholas School of the Environment, Duke University, Durham, NC 27708; <sup>b</sup>Divisions of Solid Earth Dynamics and Water, Climate and the Environment, School of Earth Sciences, The Ohio State University, Columbus, OH 43210; <sup>c</sup>School of Earth Sciences, Woods Institute for the Environment, and Precourt Institute for Energy, Stanford University, Stanford, CA 94305; <sup>d</sup>Department of Earth Sciences, Dartmouth College, Hanover, NH 03755; and <sup>e</sup>Department of Earth and Environmental Sciences, University of Rochester, Rochester, NY 14627

Edited by Thure E. Cerling, University of Utah, Salt Lake City, UT, and approved August 12, 2014 (received for review November 27, 2013)

**Horizontal drilling and hydraulic fracturing have enhanced energy production but raised concerns about drinking water contamination and other environmental impacts. Identifying the sources and mechanisms of contamination can help improve the environmental and economic sustainability of shale gas extraction. We analyzed 113 and 20 samples from drinking water wells overlying the Marcellus and Barnett Shales, respectively, examining hydrocarbon abundance and isotopic compositions (e.g., C<sub>2</sub>H<sub>6</sub>/CH<sub>4</sub>, δ<sup>13</sup>C-CH<sub>4</sub>) and providing, to our knowledge, the first comprehensive analyses of noble gases and their isotopes (e.g., <sup>4</sup>He, <sup>20</sup>Ne, <sup>36</sup>Ar) in groundwater near shale-gas wells. We addressed two questions. (i) Are elevated levels of hydrocarbon gas in drinking water aquifers near gas wells natural or anthropogenic? (ii) If fugitive gas contamination exists, what mechanisms cause it? Against a backdrop of naturally occurring salt- and gas-rich groundwater, we identified eight discrete clusters of fugitive gas contamination, seven in Pennsylvania and one in Texas, that showed increased contamination through time. Where fugitive gas contamination occurred, the relative proportions of thermogenic hydrocarbon gas (e.g., CH<sub>4</sub>, <sup>4</sup>He) were significantly higher ( $P < 0.01$ ) and the proportions of atmospheric gases (air-saturated water; e.g., N<sub>2</sub>, <sup>36</sup>Ar) were significantly lower ( $P < 0.01$ ) relative to background groundwater. Noble gas isotope and hydrocarbon data link four contamination clusters to gas leakage from intermediate-depth strata through failures of annulus cement: three to target production gases that seem to implicate faulty production casings and one to an underground gas well failure. Noble gas data appear to rule out gas contamination by upward migration from depth through overlying geological strata triggered by horizontal drilling or hydraulic fracturing.**

noble gas geochemistry | groundwater contamination | methane

**R**ising demands for domestic energy resources, mandates for cleaner burning fuels, and efforts to reduce greenhouse gas emissions are driving an energy transformation from coal toward hydrocarbon gases produced from unconventional resources (1, 2). Horizontal drilling and hydraulic fracturing have substantially increased hydrocarbon recovery from black shales and other unconventional resources (1, 2) (Fig. S1) to the extent that shale gas now accounts for more than one third of the total natural gas production in the United States (3).

Public and political support for unconventional energy extraction is tempered by environmental concerns (4, 5), including the potential for compromised drinking water quality near shale gas development (6, 7). The presence of elevated methane and aliphatic hydrocarbons (ethane, propane, etc.) in drinking water, for instance, remains controversial and requires distinguishing between natural and anthropogenic sources (6–12). Some studies have suggested that shale gas development results in fugitive gas contamination in a subset of wells near drill sites (6, 7), whereas others have suggested that the distribution of hydrocarbon gases in aquifers overlying the Marcellus Shale is natural and unrelated

to shale gas development (8, 9, 13). This study addresses two critical questions: (i) are elevated levels of hydrocarbon gas in drinking water aquifers near gas wells derived from natural or anthropogenic sources and (ii) if fugitive gas contamination exists, what mechanisms cause it?

Previous efforts to resolve these questions identify the genetic fingerprint of hydrocarbon gases using the molecular (e.g., [C<sub>2</sub>H<sub>6</sub> plus heavier aliphatic hydrocarbons]/[CH<sub>4</sub>]; abbreviated as C<sub>2</sub>H<sub>6</sub><sup>+</sup>/CH<sub>4</sub>) and stable isotopic [e.g., δ<sup>13</sup>C-CH<sub>4</sub>, δ<sup>2</sup>H-CH<sub>4</sub>, or Δ<sup>13</sup>C=(δ<sup>13</sup>C-CH<sub>4</sub>-δ<sup>13</sup>C-C<sub>2</sub>H<sub>6</sub>)] compositions of hydrocarbon gases (6–9, 13) (SI Text). These techniques resolve thermogenic and biogenic hydrocarbon contributions and differentiate between hydrocarbon sources of differing thermal maturity [e.g., Middle-Devonian (Marcellus)-produced gases vs. Upper Devonian (UD) gas pockets at intermediate depths]. However, microbial activity and oxidation can alter the original geochemical signature (14) and obscure the sources or mechanisms of fluid migration (8, 9).

Noble gas elemental and isotopic tracers constitute an appropriate complement to hydrocarbon geochemistry. Their nonreactive nature (i.e., unaffected by chemical reactions or microbial activity) (14) and well-characterized isotopic compositions in the crust, hydrosphere, and atmosphere (SI Text) make noble gases ideal tracers of crustal fluid processes (14–17). In most aquifers,

## Significance

**Hydrocarbon production from unconventional sources is growing rapidly, accompanied by concerns about drinking water contamination and other environmental risks. Using noble gas and hydrocarbon tracers, we distinguish natural sources of methane from anthropogenic contamination and evaluate the mechanisms that cause elevated hydrocarbon concentrations in drinking water near natural gas wells. We document fugitive gases in eight clusters of domestic water wells overlying the Marcellus and Barnett Shales, including declining water quality through time over the Barnett. Gas geochemistry data implicate leaks through annulus cement (four cases), production casings (three cases), and underground well failure (one case) rather than gas migration induced by horizontal drilling or hydraulic fracturing deep underground. Determining the mechanisms of contamination will improve the safety and economics of shale-gas extraction.**

Author contributions: T.H.D., A.V., R.B.J., and R.J.P. designed research; T.H.D., A.V., R.B.J., N.R.W., and R.J.P. performed research; T.H.D., A.V., R.B.J., N.R.W., and R.J.P. analyzed data; and T.H.D., A.V., R.B.J., N.R.W., and R.J.P. wrote the paper.

The authors declare no conflict of interest.

This article is a PNAS Direct Submission.

Freely available online through the PNAS open access option.

<sup>1</sup>To whom correspondence should be addressed. Email: darrah.24@osu.edu.

This article contains supporting information online at [www.pnas.org/lookup/suppl/doi:10.1073/pnas.1322107111/-DCSupplemental](http://www.pnas.org/lookup/suppl/doi:10.1073/pnas.1322107111/-DCSupplemental).

the noble gas isotopic composition reflects a binary mixture of two sources (i) air-saturated water (ASW), containing  $^{20}\text{Ne}$ ,  $^{36}\text{Ar}$ , and  $^{84}\text{Kr}$  (and  $\text{N}_2$ ) derived from solubility equilibrium with the atmosphere during groundwater recharge; and (ii) crustal rocks that release radiogenic noble gases such as  $^4\text{He}^*$  and  $^{21}\text{Ne}^*$  (sourced from  $^{235}\text{U}$ ,  $^{238}\text{U}$  +  $^{232}\text{Th}$  decay) and  $^{40}\text{Ar}^*$  (sourced from  $^{40}\text{K}$  decay, where \* indicates a radiogenic component) (18). Once noble gases incorporate into crustal fluids, they fractionate only by well-constrained physical mechanisms (e.g., diffusion, phase partitioning) (16, 18). Therefore, when paired with hydrocarbon composition and inorganic water chemistry, noble gases can help differentiate between natural geological migration of hydrocarbon gases and anthropogenic contamination. We also posit that noble gas geochemistry can be used to determine the mechanisms by which anthropogenic gas contamination occur.

We envision seven scenarios that, alone or together, can account for the elevated hydrocarbon levels in shallow aquifers (Fig. 1): (i) in situ microbial methane production; (ii) natural in situ presence or tectonically driven migration over geological time of gas-rich brine from an underlying production formation (e.g., Marcellus or Barnett Fm.) or gas-bearing formation of intermediate depth (e.g., Lock Haven/Catskill Fm. or Strawn Fm.); (iii) exsolution of hydrocarbon gas already present in shallow aquifers following scenario 1 or 2, driven by vibrations or water level fluctuations due to drilling activities; (iv) leakage from the target or intermediate-depth formations through a poorly cemented well annulus; (v) leakage from the target formation through faulty well casings (e.g., poorly joined or corroded casings); (vi) migration of hydrocarbon gas from the target or overlying formations along natural deformation features (e.g., faults, joints, or fractures) or those initiated by drilling (e.g., faults or fractures created, reopened, or intersected by drilling or hydraulic fracturing activities); and (vii) migration of target or intermediate-depth gases through abandoned or legacy wells. In our study areas, other scenarios such as coal bed methane or leakage from pipelines or compressors into aquifers are unlikely (Figs. S2 and S3).

Here, we examine the noble gas (e.g.,  $^4\text{He}$ ,  $^{20}\text{Ne}$ , and  $^{36}\text{Ar}$ ), hydrocarbon (e.g.,  $\delta^{13}\text{C}\text{-CH}_4$ ,  $\text{CH}_4$ , and  $\text{C}_2\text{H}_6$ ), and chloride ( $\text{Cl}^-$ ) content of 113 domestic groundwater wells and one natural methane seep overlying the Marcellus study area (MSA) ~800–2,200 m underground in northeastern Pennsylvania and southeastern New York and 20 groundwater wells overlying the Barnett study area (BSA) ~1,950–2,500 m underground in east-central Texas (SI Text and Figs. S2 and S3). Sample collection and analyses are reported briefly in *Materials and Methods* and in more detail in SI Text (7, 19–21). The typical depth of drinking water wells in the MSA is 35–90 m, sourced from either fractured

sandstone of the Lock Haven and Catskill Formations or outwash alluvium aquifers. The typical depth to drinking water there is 60–75 m, sourced from the Upper Trinity limestone. More geological information is included in SI Text. To augment our previous studies (6, 7) that examined the relationship between methane and proximity to gas wells, in this study we intentionally targeted a subset of water wells known to have elevated  $\text{CH}_4$  concentrations and surrounding water wells both near and far from drill sites. The reason for this approach was to distinguish among the mechanisms causing high gas concentrations naturally from those potentially associated with shale-gas development (Fig. 1).

## Results and Discussion

The occurrence, distribution, and composition of hydrocarbons in the Earth's crust result from the interplay between tectonic and hydrologic cycles (14, 17). The remnants of these processes generate inorganic, hydrocarbon, and noble gas compositions with distinctive geochemical fingerprints (e.g.,  $\text{C}_2\text{H}_6^+/\text{CH}_4$ ,  $\delta^{13}\text{C}\text{-CH}_4$ ,  $^4\text{He}/\text{CH}_4$ ,  $^{20}\text{Ne}/^{36}\text{Ar}$ , and  $\text{Cl}^-$ ) that can help to distinguish hydrocarbons that migrated naturally from those that migrated as anthropogenic fugitive gases associated with shale-gas development. Our data show that in the aquifers overlying the MSA, the  $\text{CH}_4$  levels in groundwater samples observed >1 km from shale gas wells co-occurs with elevated concentrations of natural crustal brine components (e.g.,  $\text{Cl}^-$  and  $^4\text{He}$ ) (triangles in Fig. 2A and B). Conversely, the composition of groundwater sampled <1 km from drill sites in the MSA shows clear evidence of two populations: (i) wells with compositions statistically indistinguishable from those collected >1 km from drill sites (circles in Fig. 2A and B) and (ii) wells with low salt ( $\text{Cl}^-$ ) concentrations but that are supersaturated with respect to methane and have distinct noble gas compositions (green-rimmed circles in Fig. 2A and B).

Similar to the results for methane, the noble gas compositions from groundwater samples in the MSA >1 km from shale gas wells (triangles), including the gas-rich saline spring at Salt Springs State Park north of Montrose, PA (square, Fig. 2A), and some samples <1 km from drill sites (circles, Fig. 2A) all had similar diagnostic noble gas compositions (Fig. 2A and B). These samples have  $\text{CH}_4/^{36}\text{Ar}$  at or below  $\text{CH}_4$  saturation [ $p(\text{CH}_4) \leq 1$  atm, i.e., below the “bubble point”; SI Text] and show a corresponding increase in the ratio of thermogenic gas components to ASW (i.e.,  $\text{CH}_4/^{36}\text{Ar}$  vs.  $[\text{Cl}^-]$ ,  $r^2 = 0.72$ ,  $P < 0.01$ ; and  $^4\text{He}/^{20}\text{Ne}$  vs.  $[\text{Cl}^-]$ ,  $r^2 = 0.59$ ,  $P < 0.01$ ; Fig. 2A and B). In fact, the regression of  $\text{CH}_4/^{36}\text{Ar}$  vs.  $[\text{Cl}^-]$  for all samples >1 km from gas wells (Fig. 2A) is indistinguishable from a regression of the subset of points <1 km from drill sites, suggesting one continuous population ( $P = 0.31$ , Chow test); we define these samples as the “normal trend” for brevity. These data suggest that the natural salt- and gas-rich waters in the MSA have a groundwater chemistry derived from a deep gas-rich brine that migrated over geological time (typified by the Salt Spring) and then mixed with meteoric water of ASW composition ( $[\text{Cl}^-] = <10$  mg/L;  $\text{CH}_4/^{36}\text{Ar} = \sim 0$ ;  $^4\text{He}/^{20}\text{Ne} = \sim 0.3$ ). The co-existence of elevated  $\text{CH}_4$ ,  $\text{Cl}^-$ , and  $^4\text{He}$  is consistent with previous observations for brine migration that represents a natural hydrocarbon gas source in scenario 2 (Fig. 1) (20).

A subset of samples collected <1 km from drill sites, however, shows different relationships for  $\text{CH}_4/^{36}\text{Ar}$  and  $^4\text{He}/^{20}\text{Ne}$  vs.  $\text{Cl}^-$ ; we define this subset as the “anomalous subset” for brevity. These samples show significantly higher levels of thermogenic gases ( $P < 0.01$ ) relative to ASW gases (i.e., elevated  $\text{CH}_4/^{36}\text{Ar}$  and  $^4\text{He}/^{20}\text{Ne}$ ) independent of  $[\text{Cl}^-]$  (green-rimmed circles in Fig. 2A and B). Because  $\text{CH}_4$  and  $^{36}\text{Ar}$  and  $^4\text{He}$  and  $^{20}\text{Ne}$  pairs have similar gas/liquid partition coefficient (1/solubility) ratios (SI Text), a lack of correlation between  $\text{Cl}^-$  concentrations and either  $\text{CH}_4/^{36}\text{Ar}$  or  $^4\text{He}/^{20}\text{Ne}$  ( $P = 0.864$  and  $0.698$ , respectively) suggests that the anomalous subset (Fig. 2) represents a thermogenic hydrocarbon gas that has separated from the brine-meteoric water mixture and migrated in the gas phase.

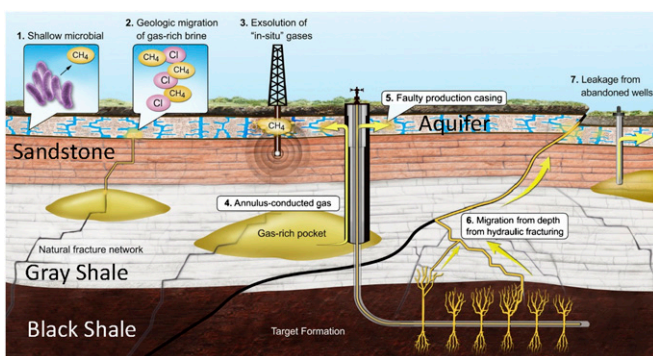


**Fig. 1.** A diagram of seven scenarios that may account for the presence of elevated hydrocarbon gas levels in shallow aquifers (see discussion in text). The figure is a conceptualized stratigraphic section and is not drawn to scale. Additional scenarios (e.g., coal bed methane and natural gas pipelines leaking into aquifers) are unlikely in our specific study areas (Figs. S2 and S3).

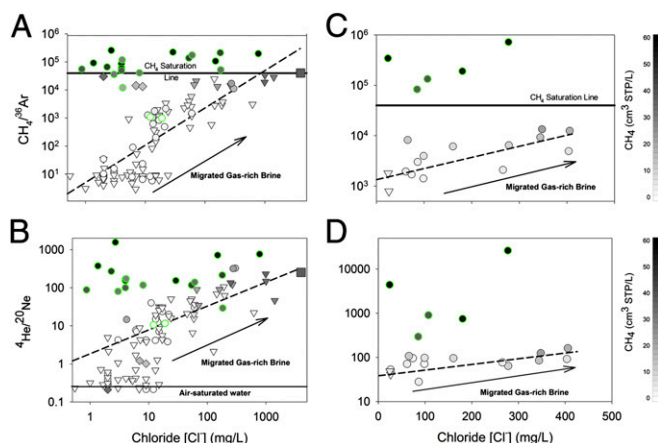


**Fig. 2.** The ratios of  $\text{CH}_4/^{36}\text{Ar}$  [ratios are in units  $(\text{cm}^3 \text{STP/L})/(\text{cm}^3 \text{STP/L})$ ; A and C] and  $^4\text{He}/^{20}\text{Ne}$  (B and D) vs.  $\text{Cl}^-$  of domestic groundwater wells. The samples were collected in the Marcellus (MSA) (Left) and Barnett (BSA) (Right) study areas at distances  $>1$  km (triangles) and  $<1$  km (circles) from unconventional drill sites.  $[\text{CH}_4]$  is shown using grayscale intensity  $[0-60^+ \text{cm}^3 ((\text{CH}_4) \text{STP/L})]$ . The dashed lines in the MSA are the regressions of all points collected  $>1$  km from drill sites. In the MSA, all samples  $>1$  km from drill sites had  $[\text{CH}_4]$  at or below saturation and showed significant correlations between  $\text{Cl}^-$  and  $\text{CH}_4/^{36}\text{Ar}$  ( $r^2 = 0.72$ ;  $P < 0.01$ ) or  $^4\text{He}/^{20}\text{Ne}$  ( $r^2 = 0.59$ ;  $P < 0.01$ ) defined as the normal trend. For samples  $<1$  km from drill sites, one subset was consistent with the "normal trend" ( $P = 0.31$ ), whereas the other anomalous subset had supersaturated  $[\text{CH}_4]$  and high  $\text{CH}_4/^{36}\text{Ar}$  and  $^4\text{He}/^{20}\text{Ne}$ , even at low  $[\text{Cl}^-]$  (green-rimmed circles in A and B). The natural Salt Spring in Montrose, PA, is shown as a square in all MSA figures, and samples targeted for microbial-sourced gases are distinguished by diamonds. In the BSA, 15 samples had  $[\text{CH}_4]$  at or below saturation and significant correlations between  $\text{Cl}^-$  and  $\text{CH}_4/^{36}\text{Ar}$  ( $r^2 = 0.59$ ;  $P < 0.01$ ) or  $^4\text{He}/^{20}\text{Ne}$  ( $r^2 = 0.48$ ;  $P < 0.01$ ) (dashed lines in C and D). Five samples, including two that changed between the first and second sampling periods (Fig. S6), had substantially higher  $\text{CH}_4/^{36}\text{Ar}$  and  $^4\text{He}/^{20}\text{Ne}$  independent of  $[\text{Cl}^-]$ . The anomalous subset of samples from both locations with elevated  $\text{CH}_4$  that do not fall along the normal trend ( $>1$  km) regression lines are consistent with a flux of gas-phase thermogenic hydrocarbon gas into shallow aquifers.

To test this geochemical framework in another shale gas basin, we compared the MSA data to those from the BSA, where the source of elevated  $\text{CH}_4$  concentrations reported in domestic water wells has been controversial (Fig. S3). Our initial sampling in December 2012 revealed that 9 of 12 BSA groundwater samples were similar to the normal trend samples from the MSA. For instance,  $[\text{CH}_4]$  and the ratios of thermogenic gas to meteoric water [i.e.,  $\text{CH}_4/^{36}\text{Ar}$  ( $r^2 = 0.59$ ;  $P < 0.01$ ) and  $^4\text{He}/^{20}\text{Ne}$  ( $r^2 = 0.48$ ;  $P < 0.01$ )] increased with  $[\text{Cl}^-]$  (triangles and circles in Fig. 2 C and D). In contrast, three domestic wells showed identical trends to the anomalous subset of samples near gas wells in the MSA, with  $\text{CH}_4/^{36}\text{Ar}$  substantially above saturation and elevated  $^4\text{He}/^{20}\text{Ne}$ , even at low  $[\text{Cl}^-]$  (green-rimmed circles in Fig. 2 C and D).

To confirm these results, we resampled 12 domestic water wells from the BSA during both August and November of 2013. The two 2013 sampling campaigns each included four additional domestic wells (8 new; 20 in total). None of the new samples showed evidence of contamination. Ten of the initial 12 samples, including the three anomalous water wells, showed similar results for the 2012 analyses (green-rimmed circles in Fig. 2 C and D and SI Text). However, by the time of our August 2013 sampling, two of the initial samples that were originally consistent with the normal trend showed increased hydrocarbon gas concentrations that coincided with greater  $\text{CH}_4/^{36}\text{Ar}$  and  $^4\text{He}/^{20}\text{Ne}$ , consistent with a transition to the anomalous subset over time (Fig. 2 C and D and SI Text). One water well showed order-of-magnitude increases of both  $\text{CH}_4/^{36}\text{Ar}$  (24,782–722,534) and  $^4\text{He}/^{20}\text{Ne}$  (267–26,324), whereas the other showed similar trends in  $\text{CH}_4/^{36}\text{Ar}$

Ar (750–81,163) and  $^4\text{He}/^{20}\text{Ne}$  (42–569) during the same period (Fig. 2 C and D and SI Text). Because the  $[\text{Cl}^-]$  did not change in either well, we suggest that thermogenic hydrocarbon gas migrated into these wells in the gas phase unaccompanied by brine between December 2012 and August 2013.

The concentrations of dissolved ASW gases (i.e.,  $^{20}\text{Ne}$ ,  $^{36}\text{Ar}$ , and  $\text{N}_2$ ) can further constrain the interactions that occur between hydrocarbon gas and water (16, 22–25). In the MSA, all normal trend samples both  $>1$  km and  $<1$  km from drill sites had  $^{36}\text{Ar}$  and  $\text{N}_2$  that varied within  $\sim 15\%$  of the temperature-dependent ASW solubility line (cyan line in Fig. 3 A–C) (25–28). Although some background ground waters showed minor excess air entrainment common in pumped groundwater globally (SI Text) (23, 29), these ranges reflect equilibration between the atmosphere and meteoric water during groundwater recharge (26, 27). In contrast, the anomalous subset of wells in the MSA (green-rimmed circles in Fig. 3 A and B) that have elevated methane and that departed from the brine-meteoric water mixing line were stripped of ASW gases compared with the expected solubility equilibria ( $P < 0.001$ ; Fig. 3 A and B).

Consistent with the results from the MSA, our data suggest that 5 water wells in the BSA display evidence of gas-phase migration associated with hydrocarbon gas extraction, whereas the remaining 15 samples appear to have acquired methane naturally. The initial December 2012 sampling identified three anomalous samples in Texas with supersaturated  $\text{CH}_4$  that departed from the brine-meteoric water mixing line (Fig. 2 C and D). Each of these samples also showed significant depletions (i.e., stripping) of all

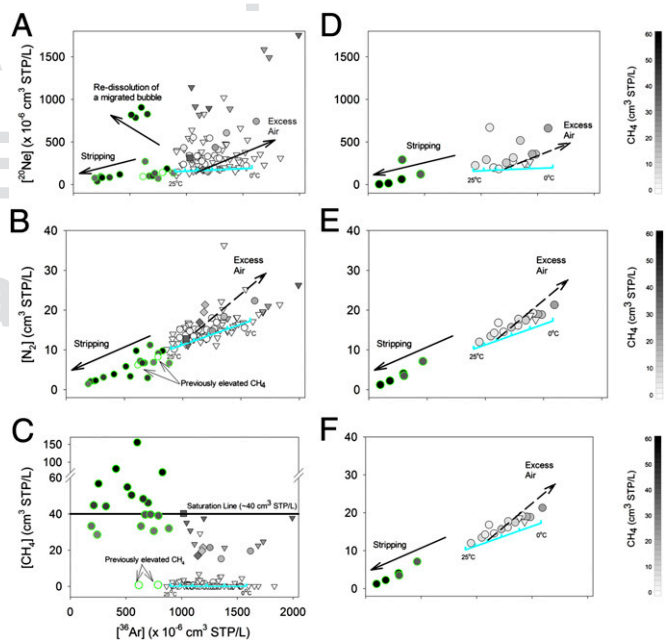


**Fig. 3.**  $^{20}\text{Ne}$  (Top),  $\text{N}_2$  (Middle), and  $\text{CH}_4$  (Bottom) vs.  $^{36}\text{Ar}$  in the MSA (Left) and BSA (Right) at distances  $>1$  km (triangles) and  $<1$  km (circles) from drill sites. All normal trend samples have  $^{36}\text{Ar}$  and  $\text{N}_2$  within 15% of the temperature-dependent ASW solubility line (cyan lines). Conversely, a subset of wells with elevated  $[\text{CH}_4]$   $<1$  km from drill sites (green-rimmed circles) shows significantly stripped ASW gases ( $^{20}\text{Ne}$ ,  $^{36}\text{Ar}$ ,  $\text{N}_2$ ), which result from extensive partitioning of dissolved ASW gases into a large volume of migrating gas-phase hydrocarbons (i.e., a fugitive gas). Note that domestic wells labeled previously elevated  $\text{CH}_4$  were vented to remove methane from the water before our sampling. Consistent with the MSA, most BSA samples (15 of 20) also have normal ASW composition, but five anomalous samples, including the two that displayed pronounced changes between the initial and later sampling events (Fig. S7), have significantly stripped ASW gas composition (green-rimmed circles).

ASW components ( $^{36}\text{Ar}$  and  $\text{N}_2$ ) (green-rimmed circles in Fig. 3 D–F). Data from our second and third sampling campaigns in August and November of 2013 reinforced these trends. The three original anomalous samples remained stripped of their ASW components, but the two previously normal wells that displayed increased  $\text{CH}_4$  through time also became depleted of ASW gases (i.e., stripped) by August 2013 and remained stripped in the November sampling (Fig. S7).

Stripped groundwater with  $^{36}\text{Ar}$  and  $\text{N}_2$  levels significantly below atmospheric solubility, similar to those that we observed in the anomalous subset of methane-rich samples from both the MSA and BSA, requires exceptional hydrogeological conditions. Gas-phase migration of  $\text{CH}_4$  (or  $\text{CO}_2$ ) can lead to the exsolution of ASW into the gas phase (14, 16, 23). However, these processes have been observed only in hydrogeological settings where tectonic (e.g., geothermal springs) or microbial (e.g., methanogenesis in rice paddies, landfills) processes drive large volumes of gas-phase migration or displace the ASW gases in the vadose zone before recharge (22, 30). Even the naturally discharging gas-rich Salt Spring in Pennsylvania has  $p(\text{CH}_4) = \sim 1$  atm and normal ASW compositions, with minor bubble nucleation only occurring near the surface as hydrostatic pressure decreases (SI Text).

Stripped ASW compositions in a subset of groundwater samples occurred exclusively <1 km from drill sites in the MSA and BSA and indicate a rapid introduction of high pressure [i.e.,  $p(\text{CH}_4) \gg 1$  atm] gas-phase hydrocarbons into shallow aquifers at a rate that exceeds groundwater flow. There are no apparent tectonic or hydrologic mechanisms to drive the migration of hydrocarbon gas at sufficient rates to strip ASW gases within shallow aquifers (<100 m) in either study area. Moreover, in both study areas, samples with stripped ASW composition contain elevated levels of aliphatic hydrocarbons ( $\text{C}_2\text{H}_6$ ,  $\text{C}_3\text{H}_8$ ;  $P < 0.01$ ) and heavy stable isotopic compositions (i.e.,  $\delta^{13}\text{C}-\text{CH}_4 = > -55\text{‰}$ ) (6–9, 13) ( $P < 0.01$ ; Fig. 4B and Fig. S5), which preclude microbial production as the source for elevated methane in shallow aquifers (scenario 1) (6, 7). Note that three wells targeted for elevated microbial methane levels in the MSA (e.g., landfills; diamond symbols in Figs. 2–4) were easily distinguished by diagnostic noble gas (e.g., low  $^4\text{He}/^{20}\text{Ne}$  and  $^4\text{He}/\text{CH}_4$ ) and hydrocarbon isotopic tracers ( $\delta^{13}\text{C}-\text{CH}_4$ ; Figs. 2B and 4B), but still retained normal ASW gas levels (Fig. 3A–C and Fig. S4). More importantly, in the MSA, the hydrocarbon composition of the anomalous subset of samples is consistent with either Marcellus-produced gases (black box in Fig. 4A and B and SI Text) or overlying UD-produced gases (pink box in Fig. 4A and B and SI Text; scenario 2), whereas BSA samples require further consideration as discussed below. The combined evidence of noble gas and hydrocarbon molecular ( $\text{C}_2\text{H}_6^+/\text{CH}_4$ ) and stable isotopic ( $\delta^{13}\text{C}-\text{CH}_4$ ) compositions for the majority of anomalous subset samples is consistent with contamination by fugitive gas migration.

By constraining the mechanisms that cause elevated hydrocarbon concentrations in drinking water near natural gas wells, we can further distinguish the presence of fugitive gas contamination. Gas-rich groundwater (>1  $\text{cm}^3$  STP/L methane) samples that fall along the normal trends for hydrocarbon levels, salts, and ASW gases ( $^{36}\text{Ar}$  and  $\text{N}_2$ ) in the MSA have  $^{20}\text{Ne}/^{36}\text{Ar}$  far above ASW equilibrium ( $\sim 0.156$ ) and  $^4\text{He}/\text{CH}_4$  well above any known thermogenic hydrocarbon gas sources in the study area (Fig. 4A). We suggest that the enriched  $^{20}\text{Ne}/^{36}\text{Ar}$  and excess  $^4\text{He}$  and  $^{20}\text{Ne}$  in these samples are remnants of relatively low  $V_{\text{gas}}/V_{\text{water}}$  conditions during the geological migration of gas-rich brine from Marcellus source rocks to conventional UD hydrocarbon traps and eventually shallow aquifers as described by scenario 2 (Fig. 1).

We hypothesize that the geological migration of hydrocarbons by scenario 2 occurred in three successive steps. First, hydrocarbon maturation in the Marcellus source rocks produced sufficient methane to generate a free gas phase, which caused the

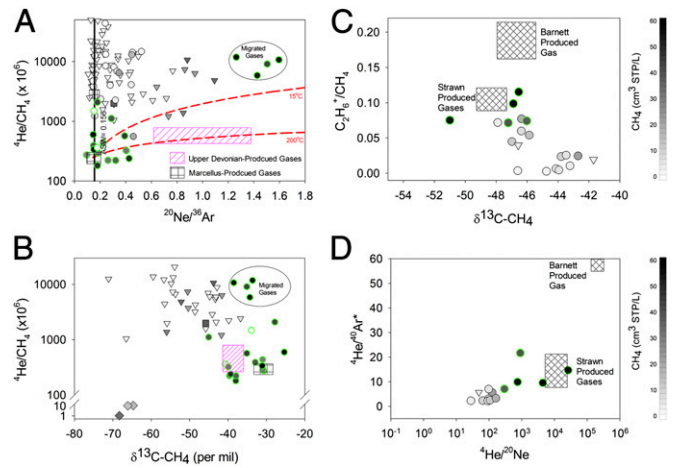


**Fig. 4.**  $^4\text{He}/\text{CH}_4$  vs.  $^{20}\text{Ne}/^{36}\text{Ar}$  (Upper Left) and  $^4\text{He}/\text{CH}_4$  vs.  $\delta^{13}\text{C}-\text{CH}_4$  (Lower Left) and  $\text{C}_2\text{H}_6^+/\text{CH}_4$  vs.  $\delta^{13}\text{C}-\text{CH}_4$  (Upper Right) and  $^4\text{He}/^{40}\text{Ar}^*$  vs.  $^4\text{He}/^{20}\text{Ne}$  (Lower Right) of produced gases and groundwater in the MSA (Left) and BSA (Right) at distances >1 km (triangles) and <1 km (circles) from drill sites. Normal trend groundwater samples in the MSA display  $^4\text{He}/\text{CH}_4$  and  $^{20}\text{Ne}/^{36}\text{Ar}$  values that increase with  $[\text{CH}_4]$  and that are significantly higher than Marcellus-produced gases. These data suggest natural geological migration of gas under relatively low  $V_{\text{gas}}/V_{\text{water}}$  conditions (scenario 2). Samples <1 km from drill sites with evidence for fugitive gas migration (green-rimmed circles) plot along a trend between Marcellus (black box) and Upper Devonian-produced gases (pink hatched box) consistent with Scenarios 4 (annulus) or 5 (production casing) (B). A cluster of groundwaters near a gas well that experienced an underground blowout (circled in A and B) displays significant stripping and enrichments in both  $^4\text{He}/\text{CH}_4$  and  $^{20}\text{Ne}/^{36}\text{Ar}$ , consistent with modeled solubility fractionation vectors (red dashed lines) for gas migration through the water-saturated crust (e.g., along faults or fractures) (scenario 6), but likely results from a well packer failure at depth (scenario 5). The Strawn- and Barnett-produced gases include data reported in ref. 8 and collected as part of the present study (Table S2). The molecular ratio of aliphatic hydrocarbons ( $\text{C}_2\text{H}_6^+/\text{CH}_4$ ) (C) and noble gases ( $^4\text{He}/^{40}\text{Ar}^*$  and  $^4\text{He}/^{20}\text{Ne}$ ) (D) in samples with evidence of fugitive gas contamination (green-rimmed circles) are significantly greater than other natural groundwaters in the area. The similarity between the  $\text{C}_2\text{H}_6^+/\text{CH}_4$ ,  $^4\text{He}/^{40}\text{Ar}^*$ , and  $^4\text{He}/^{20}\text{Ne}$  composition of the five impacted wells, including the two that changed between the first and second samplings (Fig. S8), and Strawn-produced gases, suggests an intermediate depth Strawn gas (scenario 4) as the most likely cause for the fugitive gas contamination observed in Texas.

naturally present trace gases to partition from the formational brine into the gas phase. As trace gases partition between the brine and gas phases, the degree of fractionation between trace components such as  $^{20}\text{Ne}$  and  $^{36}\text{Ar}$  (or other trace gases) is a function of the respective partition coefficients between gas and water and the relative volumes of gas and water ( $V_{\text{gas}}/V_{\text{water}}$ ; SI Text) (18). Because Ne and He have higher partition coefficients (i.e., lower solubilities in the fluid) than Ar or  $\text{CH}_4$ , this initial stage of relatively low  $V_{\text{gas}}/V_{\text{water}}$  gas-phase separation causes the enrichment of  $^{20}\text{Ne}$  and  $^4\text{He}$  in the migrating gas phase, whereas the residual Marcellus fluid becomes relatively depleted in  $^{20}\text{Ne}/^{36}\text{Ar}$  below ASW (0.10–0.12, as reported in ref. 19). In the second stage, the buoyant migration of relatively He- and Ne-enriched hydrocarbon gas into overlying formations further increases the concentration of less soluble trace gases (i.e.,  $^4\text{He}$  and  $^{20}\text{Ne}$ ) with respect to more soluble gases (i.e.,  $^{36}\text{Ar}$  and  $\text{CH}_4$ ) that will preferentially redissolve into the water-saturated crust. This redissolution process would yield elevated  $^{20}\text{Ne}/^{36}\text{Ar}$  and  $^4\text{He}/\text{CH}_4$  in the hydrocarbon gases emplaced in the overlying UD reservoirs, which is supported by the observed  $^{20}\text{Ne}/^{36}\text{Ar}$  composition of UD-produced gases (up to 1.4) in the northern Appalachian Basin (Fig. 4A) as reported in ref. 19. The final stage likely occurs at present, when hydrocarbon gases that previously migrated into UD traps (e.g., in

the Lock Haven/Catskill) diffuse into and equilibrate with overlying shallow aquifers.

In contrast to the normal trend samples that show extensive fractionation following a complex history of geological migration, all samples from the anomalous subset are located <1 km from drill sites in Pennsylvania and have noble gas compositions that are inconsistent with the geological migration of hydrocarbon gas through the water-saturated crust (scenario 2). Instead, the anomalous subset of samples has significantly lower  $^{20}\text{Ne}/^{36}\text{Ar}$  ( $P < 0.01$ ) and  $^4\text{He}/\text{CH}_4$  ( $P < 0.01$ ) than background samples (Fig. 4A). These data likely suggest that hydrocarbon gases were emplaced into the shallow aquifer without significant fractionation of ASW  $^{20}\text{Ne}/^{36}\text{Ar}$  during transport through the water-saturated crust (green-rimmed circles in Figs. 3A–C and 4A). Consequently, for the anomalous subset of groundwater samples with stripped ASW compositions, five possible mechanisms for gas migration to shallow aquifers remain plausible (scenarios 3–7; Fig. 1), all of which implicate an anthropogenic mechanism related to gas drilling and extraction. Distinguishing among these mechanisms will further clarify the environmental implications of fugitive gas contamination and lead to engineering solutions.

Elevated  $\text{CH}_4$  levels may result from the exsolution of hydrocarbon gas already present in shallow aquifers during drilling (scenario 3). This mechanism would release hydrocarbon gases that previously migrated into shallow aquifers by scenario 2 that later phase separated from brine-rich groundwater during drilling. However, this process would release hydrocarbon gases from shallow aquifers without altering the  $\text{CH}_4/^{36}\text{Ar}$  or  $^4\text{He}/^{20}\text{Ne}$  in either the migrated gas or the residual fluid because of the similar partition coefficients between the respective gases (SI Text). Because none of the data (specifically highly elevated  $\text{CH}_4/^{36}\text{Ar}$ ,  $^4\text{He}/^{20}\text{Ne}$ , and  $\delta^{13}\text{C}-\text{CH}_4$ ) from the anomalous subset of samples are consistent with scenario 2 in the MSA or BSA, we suggest that scenario 3 is unlikely.

Gas-phase leakage through scenarios 4 (well annulus), 5 (faulty casing), and 7 (legacy/abandoned wells) would transmit thermogenic gases from depth to the shallow aquifers with minimal interactions between the deep, pressurized gas-phase and static water present in stratigraphic units in the crust. As a result, the hydrocarbon gas released by these mechanisms would have high ratios of thermogenic to ASW components (i.e., high  $\text{CH}_4/^{36}\text{Ar}$  and  $^4\text{He}/^{20}\text{Ne}$ ), stripped ASW compositions and would undergo minimal fractionation of hydrocarbon gas during transport from each of the respective production intervals (e.g., Marcellus or UD formations) to shallow aquifers. As a result, the gases released through scenarios 4, 5, or 7 should also retain the composition of the gas-rich reservoir formation (i.e.,  $^4\text{He}/\text{CH}_4$ ,  $^{20}\text{Ne}/^{36}\text{Ar}$ ,  $\text{C}_2\text{H}_6^+/\text{CH}_4$ , and  $\delta^{13}\text{C}-\text{CH}_4$ ).

The majority of anomalous subset samples (i.e., green-rimmed samples) in the MSA display minimal fractionation of gas compositions (e.g., low  $^{20}\text{Ne}/^{36}\text{Ar}$  and  $^4\text{He}/\text{CH}_4$ ). These data are consistent with the anthropogenic release of a fugitive hydrocarbon gas by either scenario 4, 5, or 7 depending on location, although scenario 7 is unlikely based on the lack of legacy wells in the research area (Fig. S2). Importantly, all of these data are inconsistent with scenario 6 (direct migration of gases upward through the overlying strata following horizontal drilling or hydraulic fracturing) because in this scenario, gas/liquid partitioning would significantly fractionate the diagnostic gas isotope ratios during migration through the water-saturated crust.

In the MSA and other basins, the molecular and isotopic fingerprints of the hydrocarbon gases can distinguish between scenarios 4 (annulus leakage) and 5 (faulty casing leakage) (31, 32). For example, UD-produced gases typically have lower  $\delta^{13}\text{C}-\text{CH}_4$  (–38‰ to –44‰), normal  $\Delta^{13}\text{C}_{1-2} = <0$ , and low ethane ( $\text{C}_2\text{H}_6^+/\text{CH}_4 = <0.01$ ) (6, 7, 9) (pink box in Fig. 4B and SI Text). In contrast, Marcellus-produced gases have heavier  $\delta^{13}\text{C}-\text{CH}_4$  values (–29‰ to –35‰), reversed stable isotopic composition (i.e.,  $\Delta^{13}\text{C}_{1-2} = >0$ ),

and a higher proportion of aliphatic hydrocarbons ( $\text{C}_2\text{H}_6^+/\text{CH}_4 > 0.015$ ; black box in Fig. 4B and SI Text) (7, 9, 13). By comparing  $^4\text{He}/\text{CH}_4$  vs.  $\delta^{13}\text{C}-\text{CH}_4$  (Fig. 4B),  $\text{C}_2\text{H}_6^+/\text{CH}_4$  vs.  $\delta^{13}\text{C}-\text{CH}_4$ , or  $\delta^{13}\text{C}-\text{CH}_4$  vs.  $\Delta^{13}\text{C}_{1-2}$  (Fig. S5), we find evidence for both scenarios 4 and 5 in different locations in the MSA. Three clusters of groundwater wells with noble gas evidence for fugitive gas contamination have molecular and isotopic fingerprints that are consistent with these UD sources, whereas four clusters are consistent with a Marcellus composition (black box in Fig. 4A and B).

Similarly, in the BSA, the compositions of the five anomalous samples and the distance to legacy wells (Fig. S3) also preclude scenarios 1, 2, 3, 6, and 7. However, because the isotopic composition ( $\delta^{13}\text{C}-\text{CH}_4$ ) of both the Barnett Fm. and overlying Strawn Fm. are similar, routine analyses of hydrocarbon stable isotope compositions do not easily distinguish between scenarios 4 and 5 in this setting (8). Here, additional fingerprinting techniques [such as noble gases (19) or the molecular composition of hydrocarbons] provide a complementary approach.

Noble gases are useful tracers because the ASW compositions ( $^{36}\text{Ar}$ ,  $^{20}\text{Ne}$ ) are consistent globally and the crustal components (e.g.,  $^4\text{He}$  and  $^{40}\text{Ar}$ ) are resolvable and unaffected by oxidation or microbial activity. The radiogenic gases (i.e.,  $^4\text{He}$  and  $^{40}\text{Ar}$ ) form by the time-integrated decay of U + Th and K in the crust and are released from different lithologies as a function of temperature (SI Text) (19). As a result, the  $^4\text{He}/^{40}\text{Ar}^*$  ratio is a marker for the thermal maturity of thermogenic hydrocarbon gases (19). The similarity between  $\text{C}_2\text{H}_6^+/\text{CH}_4$  vs.  $\delta^{13}\text{C}-\text{CH}_4$  and  $^4\text{He}/^{40}\text{Ar}^*$  vs.  $^4\text{He}/^{20}\text{Ne}$  in the Strawn-produced gases and the anomalous subset of five groundwater samples in the BSA suggests that contamination likely results from the release of annulus-conducted gas sourced from the Strawn Fm. (scenario 4) rather than from the Barnett Shale (scenarios 5 or 6; Fig. 4C and D).

Unlike the seven discrete clusters of groundwater contamination discussed thus far, an eighth cluster of four groundwater samples (three water wells and one ephemeral spring) in the MSA displayed evidence of stripping and significantly elevated  $^4\text{He}/\text{CH}_4$  and  $^{20}\text{Ne}/^{36}\text{Ar}$  (green-rimmed circles in the oval in Fig. 4A). These are the only samples consistent with significant fractionation during the migration of hydrocarbon gas from depth, through water-saturated strata in the crust, and finally into the shallow aquifer (scenario 6). We propose that the composition of these samples reflects a mixture between (i) residual water previously depleted in ASW components by a large flux of migrating gas similar to the mechanism observed for other stripped samples (green-filled circles) and (ii) a hydrocarbon gas that redissolved into groundwater within shallow aquifers following extensive fractionation during transport through water-saturated strata in the crust. A natural gas production well near this sampling location experienced an “underground mechanical well failure” before our sampling (12, 33). Although our noble gas and hydrocarbon data cannot eliminate scenario 6 alone, the PA DEP reports suggest that our data likely record a casing well packer failure at depth (33), consistent with scenario 5, which permitted extensive fractionation of gas components during transport through the water-saturated crust. Thus, we find no unequivocal evidence for large-scale vertical migration of hydrocarbon gas from depth attributable to horizontal drilling or hydraulic fracturing (scenario 6).

In summary, our data demonstrate eight discrete clusters of groundwater wells (seven overlying the Marcellus and one overlying the Barnett) near shale gas drill sites that exhibit evidence for fugitive gas contamination. Three clusters of groundwater wells in the MSA are consistent with hydrocarbon gas contamination from intermediate-depth UD sources and one cluster in the BSA is likely derived from an intermediate-depth Strawn source. The most likely cause for these four cases of fugitive gas contamination is the release of intermediate-depth hydrocarbon gas along the well annulus, probably as a result of poor cementation (i.e., scenario 4). Three of the remaining four groundwater well clusters

in the MSA are consistent with the release of Marcellus-like hydrocarbon gas, presumably through poorly constructed wells (e.g., improper, faulty, or failing production casings), whereas the fourth cluster, with modified Marcellus-like production gases, surrounds the natural gas well that experienced a documented underground well failure.

In general, our data suggest that where fugitive gas contamination occurs, well integrity problems are most likely associated with casing or cementing issues. In contrast, our data do not suggest that horizontal drilling or hydraulic fracturing has provided a conduit to connect deep Marcellus or Barnett Formations directly to surface aquifers. Well integrity has been recognized for decades as an important factor in environmental stewardship for conventional oil and gas production (34, 35). Future work should evaluate whether the large volumes of water and high pressures required for horizontal drilling and hydraulic fracturing influence well integrity. In our opinion, optimizing well integrity is a critical, feasible, and cost-effective way to reduce problems with drinking water contamination and to alleviate public concerns accompanying shale gas extraction.

## Methods

All water samples in the MSA ( $n = 114$ ) and the BSA ( $n = 20$ ) were analyzed for their major gas abundance (e.g.,  $\text{CH}_4$ ,  $\text{C}_2\text{H}_6$ ,  $\text{C}_3\text{H}_8$ ,  $\text{N}_2$ ), stable isotopic composition (e.g.,  $\delta^{13}\text{C}\text{-CH}_4$ ,  $\delta^{13}\text{C}\text{-C}_2\text{H}_6$ ), chloride content, and noble gas elemental

and isotopic compositions of He, Ne, and Ar, following standard methods reported previously (7, 19–21) (*SI Text*). The analytical errors in all data plots reported here are smaller than the symbols.

Before sampling, water wells were pumped to remove stagnant water until stable values for pH, electrical conductance, and temperature were obtained. Water samples were collected before any treatment systems following standard methods (20).

A more complete review of noble gas background material and numerical modeling is included in *SI Text*. Briefly, the anticipated fractionation-driven changes in gas composition are calculated by modifying previously developed GGS-R fractionation models (16). All Bunsen solubility constants ( $\beta$ ) are calculated as a function of salinity and temperatures ranging between 15 °C and 200 °C to represent present ambient groundwater temperatures and hypothetical temperatures for the migration of a geological brine. Partition coefficients ( $\alpha = \beta_x/\beta_y$ ) were calculated as a function of temperature and salinity according to refs. 26, 27, and 36.

**ACKNOWLEDGMENTS.** We thank William Chameides, Lincoln Pratson, and Ron Perkins (Duke), Anne Carey, Berry Lyons, Frank Schwartz, and William Eymold (Ohio State University), and Robyn Hannigan (University of Massachusetts-Boston) for support and critical reviews. We also appreciate the technical support of Amanda Carey (University of Rochester) and Jon Karr and Will Cook (Duke). We thank the editor, Ray Weiss, Flip Froelich, and the anonymous reviewers for significantly improving an earlier version of the manuscript. We also thank the homeowners (R.R., F.F., T.D., J.B., and E.D.) for helping with sample collection. We acknowledge financial support from National Science Foundation EAGER (EAR-1249255), Duke University, and Fred and Alice Stanback to NSOE.

1. Tour JM, Kittrell C, Colvin VL (2010) Green carbon as a bridge to renewable energy. *Nat Mater* 9(11):871–874.
2. Kerr RA (2010) Natural gas from shale bursts onto the scene. *Science* 328(5986):1624–1626.
3. USEIA (2013) *Annual Energy Outlook 2013* (Administration USEI).
4. Ellsworth WL (2013) Injection-induced earthquakes. *Science* 341:1225–1229.
5. Petron G, et al. (2012) Hydrocarbon emissions characterization in the Colorado Front Range: A pilot study. *J Geophys Res D Atmospheres* 117:D04304.
6. Osborn SG, Vengosh A, Warner NR, Jackson RB (2011) Methane contamination of drinking water accompanying gas-well drilling and hydraulic fracturing. *Proc Natl Acad Sci USA* 108(20):8172–8176.
7. Jackson RB, et al. (2013) Increased stray gas abundance in a subset of drinking water wells near Marcellus shale gas extraction. *Proc Natl Acad Sci USA* 110(28):11250–11255.
8. Kornacki AS, McCaffrey MA (2011) *Applying Geochemical Fingerprinting Technology to Determine the Source of Natural Gas Samples Obtained from Water Wells in Parker County and Hood County* (Weatherford Laboratories, TX).
9. Molofsky LJ, Connor JA, Wylie AS, Wagner T, Farhat SK (2013) Evaluation of methane sources in groundwater in northeastern Pennsylvania. *Ground Water* 51(3):333–349.
10. Vengosh A, et al. (2014) A critical review of the risks to water resources from unconventional shale gas development and hydraulic fracturing in the United States. *Environ Sci Technol*.
11. Jackson RB, et al. (2014) The environmental costs and benefits of fracking. *Annu Rev Environ Resour* 39:39.
12. Brantley SL, et al. (2014) Water resource impacts during unconventional shale gas development: The Pennsylvania experience. *Int J Coal Geol* 126:140–156.
13. Baldassare FJ, McCaffrey MA, Harper JA (2014) A geochemical context for stray gas investigations in the northern Appalachian Basin: Implications of analyses of natural gases from Neogene-through Devonian-age strata. *AAPG Bull* 98(2):341–372.
14. Lollar BS, Ballentine CJ (2009) Insights into deep carbon derived from noble gases. *Nat Geosci* 2(8):543–547.
15. Onions RK, Ballentine CJ (1993) Rare-gas studies of basin-scale fluid movement. *Phil Trans R Soc Lond Ser A Mathemat Physical Engineer Sci* 344(1670):141–156.
16. Gilfillan SMV, et al. (2009) Solubility trapping in formation water as dominant CO<sub>2</sub> sink in natural gas fields. *Nature* 458(7238):614–618.
17. Ballentine CJ, et al. (1991) Rare-gas constraints on hydrocarbon accumulation, crustal degassing and groundwater-flow in the Pannonian Basin. *Earth Planet Sci Lett* 105(1-3):229–246.
18. Ballentine CJ, Burgess R, Marty B (2002) Tracing fluid origin, transport and interaction in the crust. *Noble Gases in Geochemistry and Cosmochemistry*, eds Porcelli D, Ballentine CJ, Wieler R, Vol 47, pp 539–614.
19. Hunt AG, Darrah TH, Poreda RJ (2012) Determining the source and genetic fingerprint of natural gases using noble gas geochemistry: A northern Appalachian Basin case study. *AAPG Bull* 96(10):1785–1811.
20. Warner NR, et al. (2012) Geochemical evidence for possible natural migration of Marcellus Formation brine to shallow aquifers in Pennsylvania. *Proc Natl Acad Sci USA* 109(30):11961–11966.
21. Darrah TH, et al. (2013) Gas chemistry of the Dallol region of the Danakil Depression in the Afar region of the northern-most East African Rift. *Chem Geol* 339:16–29.
22. Solomon DK, Poreda RJ, Schiff SL, Cherry JA (1992) Tritium and He-3 as groundwater age tracers in the Borden Aquifer. *Water Resour Res* 28(3):741–755.
23. Aeschbach-Hertig W, El-Gamal H, Wieser M, Palcsu L (2008) Modeling excess air and degassing in groundwater by equilibrium partitioning with a gas phase. *Water Resour Res* 44(8):W08449.
24. Holocher J, Peeters F, Aeschbach-Hertig W, Kinzelbach W, Kipfer R (2003) Kinetic model of gas bubble dissolution in groundwater and its implications for the dissolved gas composition. *Environ Sci Technol* 37(7):1337–1343.
25. Holocher J, et al. (2002) Experimental investigations on the formation of excess air in quasi-saturated porous media. *Geochim Cosmochim Acta* 66(23):4103–4117.
26. Weiss R (1971) Effect of salinity on the solubility of argon in water and seawater. *Deep-Sea Res* 17:721.
27. Weiss R (1971) Solubility of helium and neon in water and seawater. *J Chem Eng Data* 16:235.
28. Ingram RGS, Hiscock KM, Dennis PF (2007) Noble gas excess air applied to distinguish groundwater recharge conditions. *Environ Sci Technol* 41(6):1949–1955.
29. Heaton THE, Vogel JC (1981) Excess air in groundwater. *J Hydrol (Amst)* 50(1-3):201–216.
30. Dowling CB, et al. (2002) Geochemical study of arsenic release mechanisms in the Bengal Basin groundwater. *Water Resour Res* 38(9).
31. Rowe D, Muehlenbachs K (1999) Isotopic fingerprints of shallow gases in the Western Canadian Sedimentary Basin: Tools for remediation of leaking heavy oil wells. *Org Geochem* 30:861–871.
32. Tilley B, Muehlenbachs K (2012) Fingerprinting of gas contaminating groundwater and soil in a petroliferous region, Alberta, Canada. *Environmental Forensics, Proceedings of the 2011 INEFF Conference* (RSC Publishing), pp 115–125.
33. Krancer ML (2012) *DEP Statement on Leroy Township Gas Migration Investigation* (Protection PDoE).
34. Davies RJ, et al. (2014) Oil and gas wells and their integrity: Implications for shale and unconventional resource exploitation. *Mar Pet Geol*.
35. Brufatto C (2003) From mud to cement-building gas wells. *Oilfield Review* 15:62–76.
36. Smith SP, Kennedy BM (1982) The solubility of noble gases in water and in NaCl brine. *Geochim Cosmochim Acta* 47:503–515.